Organic-matter loading determines regime shifts and alternative states in an aquatic ecosystem

Jennie Sirota[a], Benjamin Baiser[b], Nicholas J. Gotelli[c], and Aaron M. Ellison[b,1]

[a]Department of Biological Sciences, North Dakota State University, Fargo, ND 58102; [b]Harvard Forest, Harvard University, Petersham, MA 01366; and [c]Department of Biological Sciences, University of Vermont, Burlington, VT 05405

Edited by Stephen R. Carpenter, University of Wisconsin, Madison, WI, and approved April 2, 2013 (received for review December 4, 2012)

Slow changes in underlying state variables can lead to "tipping points," rapid transitions between alternative states ("regime shifts") in a wide range of complex systems. Tipping points and regime shifts routinely are documented retrospectively in long time series of observational data. Experimental induction of tipping points and regime shifts is rare, but could lead to new methods for detecting impending tipping points and forestalling regime shifts. By using controlled additions of detrital organic matter (dried, ground arthropod prey), we experimentally induced a shift from aerobic to anaerobic states in a miniature aquatic ecosystem: the self-contained pools that form in leaves of the carnivorous northern pitcher plant, *Sarracenia purpurea*. In unfed controls, the concentration of dissolved oxygen ($[O_2]$) in all replicates exhibited regular diurnal cycles associated with daytime photosynthesis and nocturnal plant respiration. In low prey-addition treatments, the regular diurnal cycles of $[O_2]$ were disrupted, but a regime shift was not detected. In high prey-addition treatments, the variance of the $[O_2]$ time series increased until the system tipped from an aerobic to an anaerobic state. In these treatments, replicate $[O_2]$ time series predictably crossed a tipping point at ~45 h as $[O_2]$ was decoupled from diurnal cycles of photosynthesis and respiration. Increasing organic-matter loading led to predictable changes in $[O_2]$ dynamics, with high loading consistently driving the system past a well-defined tipping point. The *Sarracenia* microecosystem functions as a tractable experimental system in which to explore the forecasting and management of tipping points and alternative regimes.

Regime shifts are rapid, often unexpected shifts in the dynamics of a system caused by slow, usually directional changes in an underlying state variable (1, 2). In common use, regime shifts reflect a shift from a more "desirable" state of the system to a less desirable one (3, 4). Regime shifts have been observed in a wide range of financial, physical, and biological systems (4), and accurate predictions and methods to avert tipping points and ameliorate the negative effects of regime shifts or even reverse them is a central focus of contemporary research in many fields (4–7).

A classic example of an ecological regime shift of broad societal concern is the shift from a clear, oligotrophic lake to a murky, eutrophic one. The basic mechanism of eutrophication is well understood (2, 3). Increases in limiting nutrients, especially nitrogen and phosphorous (8), boost primary production by algae and phytoplankton (9). This increase in producer biomass cannot be controlled by grazers, leading to increased shading and turbidity (10). Oxygen levels decrease as microbes decompose this biomass, often leading to population declines of grazers and predators and the collapse of aquatic "green" (i.e., producer-controlled) food webs (11). A similar sequence can occur if there is an excess of allochthonous inputs of organic matter (detritus) into "brown" (i.e., donor-controlled) aquatic ecosystems (12).

A key feature of regime shifts is that feedbacks among state variables (3, 13) and relationships between state variables or "drivers" (e.g., carbon, nitrogen, phosphorus, or other critical energy or nutrient sources) and measured response variables [e.g., turbidity, dissolved O_2 concentration ($[O_2]$), or food-web structure] can differ dramatically before and after a state change (14). For example, in oligotrophic lakes, concentrations of nitrogen and phosphorus are well correlated with producer biomass, but these correlations break down in eutrophic lakes (15). In oligotrophic lakes, excess phosphorus is absorbed by benthic sediments and its release back into the water column is slow (16). However, if the concentration of P in the water is continuously elevated, it can cross a threshold—a tipping point—beyond which the rate of P recycling between lake sediments and the water column increases rapidly (16), leading to eutrophication. However, subsequent reductions of P in the water of eutrophic lakes do not shift the lake back to an oligotrophic state because, in the eutrophic state, P recycling no longer uniquely controls the state of the system (17).

A large body of theoretical work has identified a number of statistical early-warning indicators for a tipping point, defined as the point in time when a system shifts from one regime to another (7). Less attention has been paid to systematic changes in the dynamics of systems on either side of a tipping point (8), although demonstration that alternative states exist in a system is necessary to reliably conclude that a tipping point has been passed (14). The emphasis on tipping points is perhaps unsurprising because, if a tipping point can be detected far enough in advance, a regime shift may be averted (3–6). However, modeling studies have shown that the lead time required to avert a regime shift can be unacceptably long (5, 6), so additional attention must be paid to understanding dynamics before and after state changes as a first step toward determining how to manage or reverse them (e.g., refs. 18, 19). The now-standard retrospective analyses of lengthy time series of observational data can identify tipping points, illustrate that an early warning was available if it had been looked for, and document alternative states (1, 3, 4, 20). Prospective forecasting, however, requires a different approach.

Experimental induction of regime shifts would provide a workable platform from which researchers could generate detailed knowledge of initial and final states and the tipping point in between them. An experimental system also would facilitate the development, testing, and analysis of early-warning indicators of tipping points, prospective interventions to delay or prevent regime shifts, and methods to shift the system between alternative states. Unfortunately, such experiments are rare (2), and mathematical modeling of tipping points and regime shifts has far outpaced available empirical data (7, 21). However, three recent microcosm studies have experimentally induced tipping points in populations of single species of microorganisms and tested whether "critical slowing down" (CSD) of population density indicates a rapidly

---

Author contributions: N.J.G. and A.M.E. designed research; J.S. and B.B. performed research; J.S., B.B., and A.M.E. analyzed data; and J.S., B.B., N.J.G., and A.M.E. wrote the paper.

The authors declare no conflict of interest.

This article is a PNAS Direct Submission.

Data deposition: The data reported in this paper have been deposited in the Harvard Forest Data Archive (Long Term Ecological Research) Data Archive, http://harvardforest.fas.harvard.edu/data-archive (dataset HF205).

[1]To whom correspondence should be addressed. E-mail: aellison@fas.harvard.edu.

This article contains supporting information online at www.pnas.org/lookup/suppl/doi:10.1073/pnas.1221037110/-/DCSupplemental.

approaching tipping point (22–24). These studies revealed that signals of a tipping point could be detected as early as eight generations before a transcritical threshold was crossed (22), that systemic stochasticity could reduce the signal-to-noise ratio in early-warning indicators of tipping points (23), and that fold bifurcations in system dynamics occurred as a catastrophic threshold between different system states was crossed (24). Although consistent with theoretical predictions, these studies on single species in highly simplified environments are not easily extrapolated to more complex ecosystems, such as eutrophic lakes or ponds.

In this study, we experimentally induced a tipping point and a regime shift from an aerobic to an anaerobic state in an entire aquatic ecosystem: the aquatic assemblage of microbes and invertebrates found in the leaves of the northern pitcher plant, *Sarracenia purpurea* L. (25). This *Sarracenia* "microecosystem" is ideal for studying tipping points and regime shifts for three reasons. First, it is a naturally occurring yet tractable and replicable experimental system in which water-filled pitchers host a well-characterized, five-trophic level, detritus-based food web (26, 27). Second, its carbon (photosynthetic) and nutrient-cycling dynamics are well characterized and understood (28–30), so mechanistic linkages can be made between organic-matter loading (i.e., prey addition) and persistence of, or transitions between, aerobic and anaerobic states (*SI Appendix, A Model of the* Sarracenia *System*). Finally, because it naturally exists in aerobic and anaerobic states, the *Sarracenia* system can be viewed as a model system for understanding eutrophication in freshwater ponds and lakes, which have provided some of the best examples of tipping points and regime shifts. Most systems studied so far, including the *Sarracenia* system, can shift between regimes or eventually recover from apparently catastrophic shifts (19). Moreover, our perception of the apparent long-term stability of many systems may not reflect the underlying drivers of system change (14). For these reasons, we avoid here the use of the word "stable" in "alternative stable state," and instead focus on the statistical properties of systems that emerge from controlled and replicated experiments.

Sarracenia Microecosystem

S. purpurea is a widespread, long-lived, perennial, North American carnivorous plant (31). The plant has pitcher-shaped leaves that open during the growing season, fill with rainwater, and capture invertebrate prey, primarily ants (32). This resource base of captured prey supports a five-trophic level food web that includes bacteria, protozoa, the bdelloid rotifer *Habrotrocha rosa* Donner, and larvae of several obligate Diptera (25, 33, 34). The *Sarracenia* food web has been characterized as a processing chain commensalism (33), but the top predators in the system—larvae of the pitcher plant mosquito, *Wyeomyia smithii* (Coq.), and the pitcher plant flesh-fly, *Fletcherimyia fletcheri* (Aldrich)—are not critical for breakdown of prey and translocation of nutrients to the plant; the microbes by themselves efficiently decompose and mineralize nearly all of the captured prey biomass (29).

Depending on the photosynthetic activity of the plant, the quality and quantity of captured prey, and the structure of the food web within the pitcher, the oxygen content of the liquid in pitcher in the field can vary greatly from well-oxygenated to nearly anaerobic (*SI Appendix, A Model of the* Sarracenia *System*). In aerobic conditions, captured prey is rapidly shredded by larvae of the pitcher plant midge *Metriocnemus knabii* Coq. and subsequently processed by aerobic bacteria whose populations are regulated by higher trophic levels in the food web (35). The respired carbon dioxide from the food web is taken up by the plant, which in turn releases oxygen back into the water as it photosynthesizes (28). In contrast, anaerobic conditions occur following a rapid accumulation of excess prey (often from a single pulsed input; e.g., ref. 36) that cannot be processed with sufficient speed by the animal food web (*SI Appendix*, Fig. S2). The daily input of O_2 to the aquatic microecosystem from plant photosynthesis and diffusion from the atmosphere cannot compensate for the slower breakdown of prey by anaerobic microbes, and concentration of dissolved O_2 remains at persistent low levels. In other words, when prey input is excessive, the *Sarracenia* ecosystem resembles lakes, streams, estuaries, and other aquatic ecosystems that have experienced increased biological oxygen demand following eutrophication (9, 11, 12).

Results and Discussion

In unfed controls, $[O_2]$ (expressed in percent, where percent O_2 in the atmosphere = 20.95 ≡ 1.26 g/L O_2 at 25 °C at Harvard Forest, 334 m above sea level) in all replicates exhibited a regular diurnal cycle associated with daytime photosynthesis and nocturnal plant respiration (Fig. 1*A* and *SI Appendix*, Fig. S1). In all of these control time series, there also was a slight trend toward increasing $[O_2]$ over the course of each 4-d experiment (*SI Appendix*, Fig. S6). In the two lowest prey-addition treatments (0.125 mg·mL^{-1}·d^{-1} or 0.25 mg·mL^{-1}·d^{-1} added prey), diurnal cycles of $[O_2]$ became irregular and illustrated a complex pattern of fluctuations (Fig. 1 *B* and *C*). At the two highest prey-addition treatments (0.5 mg·mL^{-1}·d^{-1} or 1.0 mg·mL^{-1}·d^{-1} added prey), the diurnal cycle of $[O_2]$ was restored, albeit with a greatly diminished amplitude and at a substantially lower overall $[O_2]$ level (Fig. 1 *D* and *E*). The frequency distribution of daytime $[O_2]$ was distinctly multimodal (Fig. 2), and depended on prey additions, not photosynthetically active radiation (PAR), which was unimodal with a single daytime mode of 388 μmol·m^{-2}·s^{-1} (*SI Appendix*, Figs. S10–S12 and Table S2). As in many other systems, these prominent modes are most parsimoniously explained as resulting from nonlinear responses of the pitcher plant microecosystem to variation in prey availability and its subsequent decomposition (*SI Appendix, Analysis of Frequency Distribution of Daytime Oxygen Concentration*). In short, experimental additions of organic-matter created and sustained aerobic and anaerobic states, and initiated a transition from aerobic to anaerobic states.

A loess model effectively detrended and decycled the control time-series data of $[O_2]$, yielding nearly constant residuals in these time series (Fig. 1*F* and *SI Appendix*, Figs. S13–S16). The $[O_2]$ time series of all prey-addition treatments still exhibited some periodicity relative to the controls (Fig. 1 *G*–*J*), but quantitative analysis of structural changes between different regimes in each time series revealed statistically significant break points only in the two highest prey-addition treatments (0.5 mg·mL^{-1}·d^{-1} and 1.0 mg·mL^{-1}·d^{-1} added prey). In each of these two treatments, tipping points were detected in five of six replicates (temporal locations of individual time series indicated by the vertical cyan lines in Fig. 1 *I* and *J*; break points of the averaged time series indicated by vertical red lines in Fig. 1 *I* and *J*). The break point in the two highest prey-addition treatments occurred, on average, 44.6 h after the start of the feeding experiment and differed between treatments on average by only 114 min [$t_{(4)} = 0.8655$; $P = 0.4$, paired *t* test], despite a doubling of the food addition rate. These results suggest that there is a threshold concentration of organic-matter loading at ~0.5 mg·mL^{-1}·d^{-1} that can reliably induce a tipping point and regime shift in the *Sarracenia* microecosystem.

In addition to differences in time-series dynamics, the statistical moments and trends of the $[O_2]$ time series differed significantly among the four prey-addition treatments and the controls (Fig. 3 and Table 1). With increasing prey addition, there were decreases in the skewness and temporal trends of $[O_2]$ (Fig. 3), and the variance of the $[O_2]$ time series increased with increasing prey additions until the system shifted from an aerobic to an anaerobic state (*SI Appendix*, Fig. S16). Within the 0.5 mg·mL^{-1}·d^{-1} prey-addition treatment—the lowest feeding level for which we observed a state change—the time-series mean was significantly higher [$t_{(5)} = 8.84$; $P < 0.001$] before the regime shift than afterward, and the temporal trend in $[O_2]$ shifted from declining before the system shifted from aerobic to anaerobic to flat after the

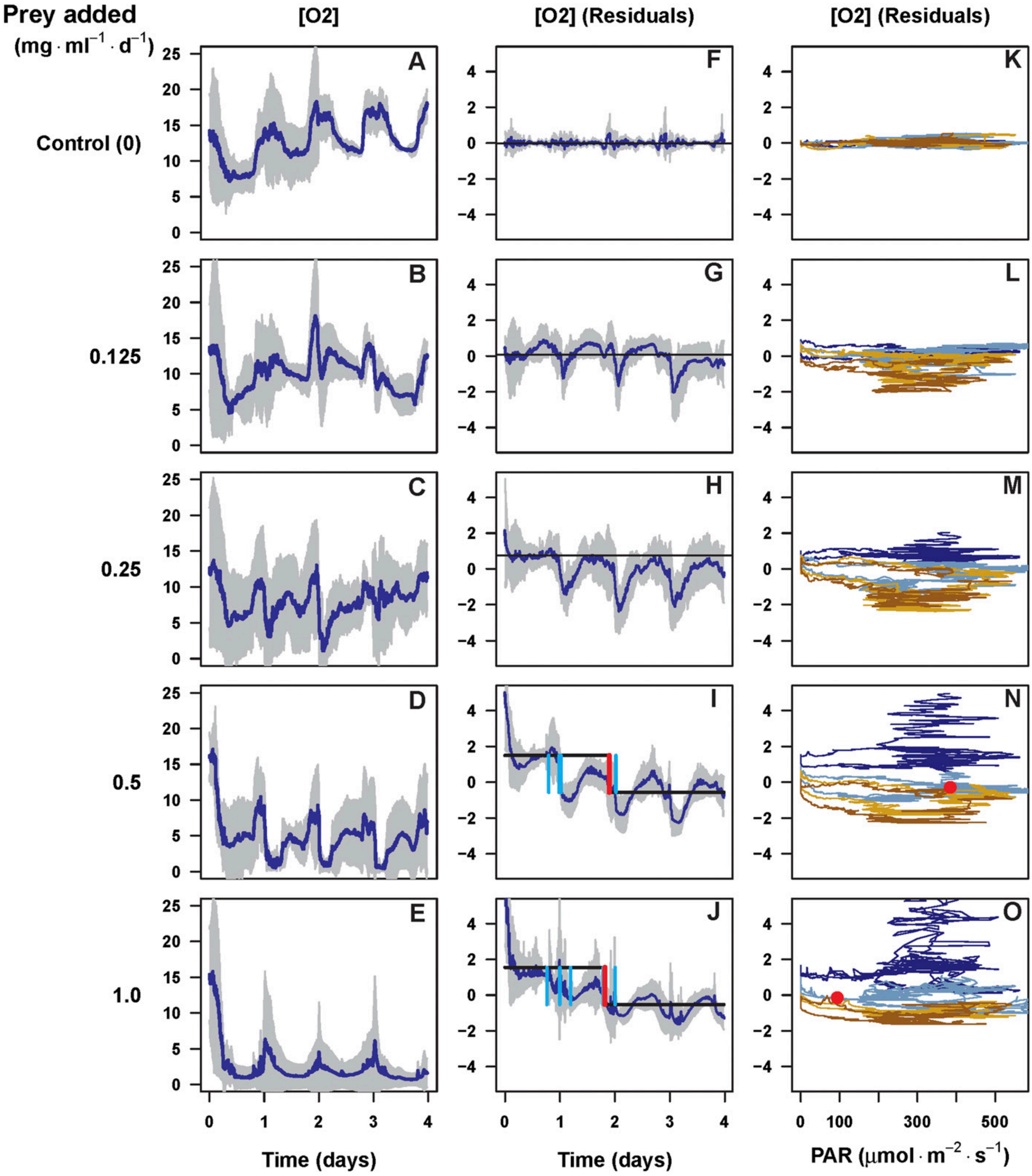

Fig. 1. Analysis of the time series of $[O_2]$ concentration (in percent; on this scale, atmospheric $[O_2] = 20.95 \equiv 1.26$ g/L in our greenhouse) in *Sarracenia* microecosystems as a function of experimental organic-matter loading through prey addition: 0 (control), 0.125, 0.25, 0.5, or 1.0 mg·mL^{-1}·d^{-1} dry mass of ground wasps ($n = 5{,}734$ observations of $[O_2]$ per replicate within each treatment). (*A*–*E*) Mean raw data $[O_2]$ time series (blue line) and 95% CIs (gray region) for each treatment across six replicates. (*F*–*J*) Mean decycled and detrended time series (blue line) and 95% CIs (gray region) for each treatment across six replicates. The five vertical cyan lines show the break points for the $[O_2]$ residuals of each replicate (one of the six replicates did not display a significant break point); the vertical red line in each treatment shows the break point for the mean of all of the series within a treatment. (*K*–*O*) Relationships between the primary environmental driver (PAR, in μmol·m^{-2}·s^{-1}) and average (residual) $[O_2]$. Lines of different colors correspond to the 4 d of each trial run: dark blue represents day 1, light blue represents day 2, yellow represents day 3, and brown represents day 4. The red circles in *N* and *O* indicate the times of the switches from aerobic to anaerobic states in the two highest prey-addition treatments.

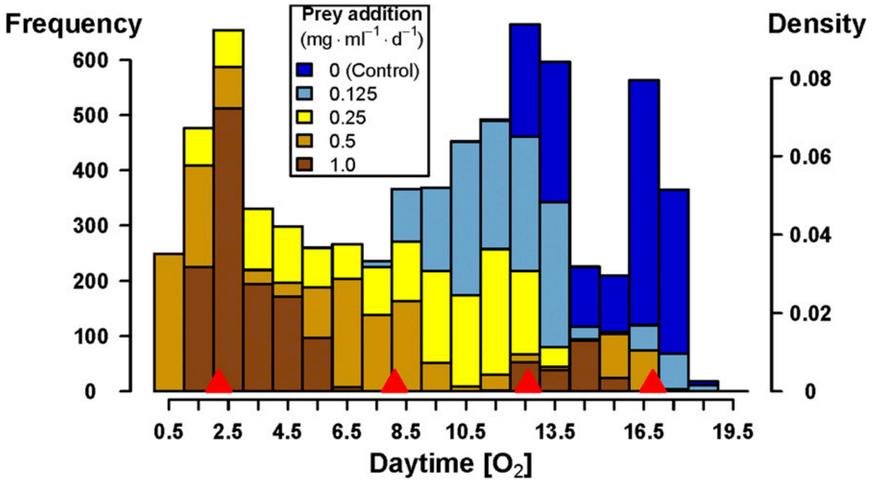

Fig. 2. Frequency distributions (number of minutes between 0900 and 1500 hours) of [O$_2$] in the five different prey-addition treatments. The red triangles indicate the locations of four modes in the joint distribution identified with normal mixture modeling and model-based clustering (*SI Appendix*, Fig. S12). The first identified mode (at 1.682% O$_2$) corresponds to the mode for the distributions of the two highest prey-addition treatments (0.5 and 1.0 mg·mL^{-1}·d^{-1}); the second (7.554%) corresponds to the mode of the distribution of the intermediate prey-addition treatment (0.25 mg·mL^{-1}·d^{-1}); the third (12.146%) corresponds to the mode for the lowest prey-addition treatment (0.125 mg·mL^{-1}·d^{-1}); and the fourth (16.272%) corresponds to the mode for the distribution of the controls.

regime shift [$t_{(5)} = 3.76$; $P = 0.007$; compare colored box plots in Fig. 3]. A statistically stronger, but qualitatively similar, result was found in the 1.0 mg·mL^{-1}·d^{-1} prey-addition treatment: all three statistical moments were higher, and the temporal trend in [O$_2$] was significantly more negative, before the regime shift than after it [mean, $t_{(5)} = 7.28$; $P < 0.001$; variance, $t_{(5)} = 5.46$; $P = 0.001$; skewness, $t_{(5)} = 4.93$; $P = 0.002$; slope, $t_{(5)} = 3.39$; $P = 0.01$]. We note, however, that these patterns do not necessarily indicate CSD. Deterministic dynamics could cause manipulated microecosystems to simply diverge further from the controls, leading to an increase in variance that would be unrelated to CSD. Thus, evidence for CSD would be better identified from analysis of individual time series or of replicate time series within each treatment (*SI Appendix*, *Supplemental Analysis of Time-Series Data*).

The relationship between [O$_2$] and light available for photosynthesis—the primary driver of O$_2$ production by the plant—differed between the two states (Fig. 1 *K*–*O* and *SI Appendix*, Figs. S13 and S14). In the unfed controls, the trajectory in phase space was virtually identical for all 4 d of the time series (Fig. 1*K*), and illustrated normal diurnal cycling of photosynthesis and respiration. As the prey-addition rate was increased, the replicated trajectories became more separated for the early and later parts of each time series (Fig. 1 *L* and *M*). At the two highest feeding levels, the different regimes were distinctly separated (either side of the red circle in Fig. 1 *N* and *O*). Such changes in the relationships between drivers and response on either side of a tipping point are consistent with theoretical and empirical studies of alternative states in ecological systems (14, 18, 19).

Conclusions

The results presented here illustrate that, with modest organic-matter loading, we can predictably induce a regime shift in a fully functioning, multitrophic, detritus-based (i.e., donor-controlled) ecological system. Although there was some variability between replicate ecosystems receiving the same prey additions, the variance within treatments was relatively small, and the system responded in characteristic and repeatable ways to increases in the feeding rate (Figs. 1 and 2 and *SI Appendix*, Figs. S12 and S14). These results suggest that organic-matter loading not only triggers the state change from the aerobic to the anaerobic state, but that decomposition of prey (35) and biological oxygen demand are the primary drivers that control the dynamics before and after a tipping point (Fig. 3 and *SI Appendix*, Figs. S3 and S7–S9).

The experimental induction of alternative states in the *Sarracenia* microecosystem provides some support for theoretical predictions of increasing variance in time series before a regime shift. More importantly, however, this study highlights the possibilities of a tractable experimental system with which to explore tipping points, regime shifts, and alternative states. Future work with this system will involve the identification of biologically based early-warning indicators of tipping points. We hypothesize that such biomarkers, including genomic and proteomic markers derived from microbial activity (37), can provide more lead time for intervention than measurements of traditional environmental variables such as [O$_2$], which may be easier to measure but are themselves driven by underlying biological processes.

Materials and Methods

We explored the dynamics of aerobic to anaerobic state changes in the pitcher plant system by using mathematical modeling (*SI Appendix*, *A Model of the Sarracenia System*) and a controlled greenhouse experiment. Replicate *S. purpurea* pitchers were inoculated with liquid collected from field plants that contained the naturally occurring bacterial community. We then varied the prey fed to each pitcher and continuously monitored [O$_2$]. Each individual *Sarracenia* leaf functioned as an independent ecosystem in which the response of an environmental variable ([O$_2$]) was monitored as a function of an environmental driver (organic-matter addition). We report [O$_2$] as a percentage, e.g., the percent O$_2$ in the atmosphere is 20.95. The greenhouse at Harvard Forest in which we did the experiment is at 334 m above sea level, where the atmospheric pressure is 0.964 that of sea level. Thus, the atmospheric density of O$_2$ in the greenhouse at 25 °C (within 0.5 °C of the average air and pitcher-fluid temperatures during the experiment, as detailed later) is 1.26 g/L.

Experimental Treatments. Pitcher plants were purchased from Meadowview Biological Station (Woodward, VA) in 2010, and maintained in the Harvard Forest greenhouse for 2 y before the experiments were initiated in June 2012. For each of six experimental trials, we randomly selected five plants and used the most recent fully formed pitcher (leaf) on each plant as the focal pitcher for a randomly assigned treatment. We filled the focal pitcher on each plant with pitcher fluid collected on the first day of each trial from pitchers growing in a naturally occurring *S. purpurea* population at Tom Swamp Bog in Petersham, MA (42°30′ N, 72°11′ W), 6 km from the greenhouse. To remove macrobes and debris larger than 30 μm in diameter, pitcher fluid was filtered first through sterile Whatman filter paper, and then through sterile Poly-Prep chromatography columns (Bio-Rad Laboratories). Focal pitchers were filled to

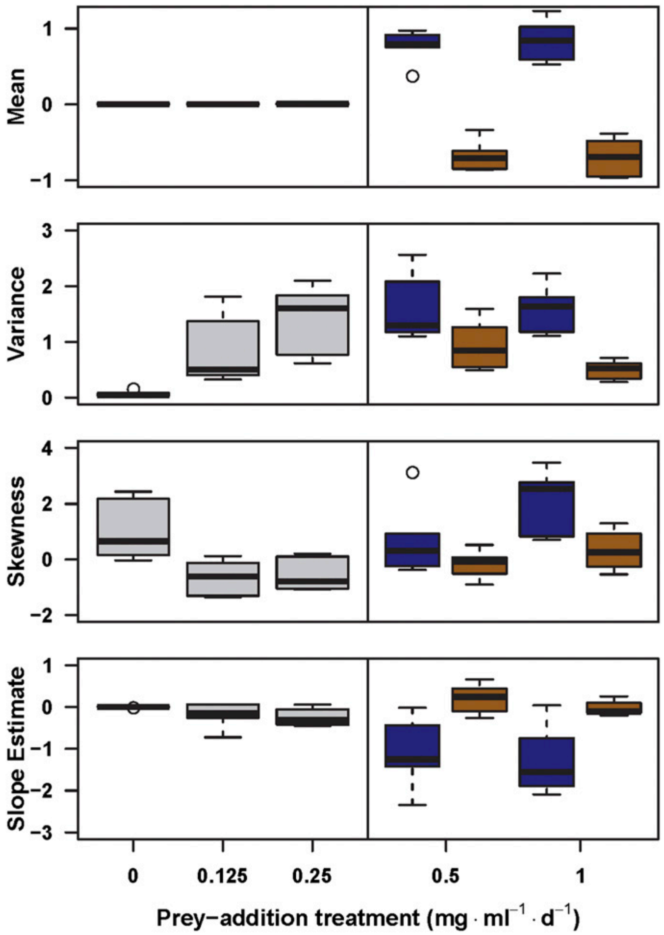

Fig. 3. Box plots of statistical moments and least-squares regression slope coefficients of the time series of [O_2]. Gray boxes represent replicates from treatments with no break points (0, 0.125. 0.25 mg·mL^{-1}·d^{-1} added prey). Blue and brown boxes represent the values for these variables in each of the two different states of the system induced by the higher levels of organic-matter loading (0.5 and 1.0 mg·mL^{-1}·d^{-1} added prey). Table 1 shows statistical summaries of treatment effects.

slightly below their rim with homogenized filtrate. Focal pitchers varied in volume from 4 mL to 18 mL, and the volume of pitcher fluid dispensed into each leaf was recorded. Nonfocal pitchers on each plant were filled with deionized water.

At 12 noon each day for four consecutive days, treated plants were fed an aliquot (0.125, 0.25, 0.5, or 1.0 mg·mL^{-1}·d^{-1}) of dried, finely ground vespid wasp [*Dolichovespula maculata* (Fabr.)] tissue that has a percentage C of 51.5, a C:N ratio of 5.99:1, and N:P:K ratios (10.7:1.75:1.01) nearly identical to those of ant species (C:N, 5.9; N:P:K, 12.1:1.52:0.93) that are the most common prey item of pitcher plants (30). The [O_2] in the pitcher fluid was measured at 1-s intervals with D-166MT-1S microelectrodes (Lazar Research Laboratories); 1-min averages were recorded with a CR-1000 data logger (Campbell Scientific). Each day when the plants were fed, oxygen electrodes were recalibrated in accordance with the manufacturer's instructions. Temperature in the pitcher fluid and the surrounding air were measured simultaneously with thermistors (mean air temperature, 25.45 °C; mean water temperature, 25.18 °C), and PAR (in μmol·m^{-2}·s^{-1}) was measured 5 cm below the tops of the plants with an LI-190SA PAR sensor (Li-COR).

We ran six of these 4-d experimental trials. Each run consisted of five plants assigned randomly to one of five different prey-addition levels (0 [unfed controls], 0.125, 0.25, 0.5, and 1.0 mg·mL^{-1}·d^{-1}) and represented a temporal block to control for unmonitored changes in the greenhouse environment through the course of the summer. Plants were assigned randomly to treatments, interspersed randomly in trays on greenhouse tables, and treated identically in all respects other than the prey-addition level they received. Total sample size over the six replicate temporal blocks was 30 plants.

Table 1. Results of randomized-block ANOVA on effects of prey addition on each of four statistical moments and linear trend of time series of [O_2]

Metric/variable	SS	df	*F*	*P* ≤ *F*
Mean				
Trial (block)	0.002	5	1.78	0.92
Prey addition	0.0002	4	0.22	0.16
Residuals	0.92	20	—	—
Variance				
Trial (block)	0.69	5	0.51	0.77
Prey addition	12.13	4	11.16	<0.001
Residuals	5.43	20	—	—
Skewness				
Trial (block)	1.93	5	0.62	0.68
Prey addition	21.99	4	8.87	<0.001
Residuals	12.40	20	—	—
Kurtosis				
Trial (block)	123.84	5	1.65	0.19
Prey addition	237.43	4	3.95	0.02
Residuals	300.65	20	—	—
Trend				
Trial (block)	0.21	5	0.92	0.49
Prey addition	2.11	4	11.41	<0.001
Residuals	0.92	20	—	—

There was no significant block (i.e., trial) effect on any of the test statistics (Table 1).

Data Analysis. For each of the 30 plants, we generated a time series of 1-min averages of [O_2] and PAR; lengths of the time series ranged from 5,734 to 5,862 observations. To facilitate averaging across replicates, we truncated the terminal observations in each series to match the shortest time series (5,734 min). During daily feeding and recalibration, the [O_2] series was interrupted; we used linear interpolation to fill in these missing values, which constituted <2% of each time series.

Statistical detection and analysis of tipping points and alternative states normally is done on detrended and decycled time series of standardized data (7). We centered and scaled individual measurements x_i ($i = 1$ to t; $t = 5{,}734$) of [O_2] in each time series as $z_i = \frac{X_i - \bar{X}}{\sigma_x}$. In time-series analyses, data are typically detrended and decycled by fitting smoother functions to a series and then calculating residuals from the fitted trend line (38). In this study, however, the control time series represents the explicit null hypothesis against which state changes caused by organic-matter additions are properly measured. Thus, rather than detrending each time series in isolation, for comparative purposes, we detrended the time series of data from the prey-addition treatments relative to the time-series data from the control plant within each block. Detrending against the controls is important because, in the absence of organic-matter loading, the [O_2] series for the *Sarracenia* microecosystem exhibits diurnal periodicity (Fig. 1*A*), reflecting the daily cycle of plant photosynthesis and respiration (28). Such periodicity can obscure early-warning indicators of tipping points (39). We fit a smoothed local regression model to each of the standardized control series by using the loess function in the stats library of R (version 2.13.1). We then decycled and detrended data from the enriched series by subtracting the predicted (loess) values of the standardized control time series from the observed, standardized values of each time series of fed pitchers. Alternative analyses of the raw time series and of time series that were detrended and decycled individually (as opposed to relative to the controls) are presented in *SI Appendix, Supplemental Analysis of Time-Series Data*. These supplemental analyses gave results that were qualitatively similar to those based on a detrending of each food-addition time series relative to the control series.

We used the strucchange library in R (40) to test statistically for the presence of break points in each of the time series (including the controls). strucchange should be applied to detrended, decycled series; a time series without breaks is flat (i.e., slope of 0) and has mean (i.e., intercept) of 0. strucchange then applies a moving window across a time series to identify the optimal number of break points (i.e., change in intercept) on the basis of the residual sum of squares and Bayesian information criterion; the latter imposes a penalty for the identification of multiple break points, and the optimal number of break points may equal 0. We used a conservative 2-SD criterion to distinguish statistically significant break points (14). Break points were identified for time series only in the two highest prey-addition treatments, and for these we used a simple *t* test to compare the average time to the break point.

Following the approach of Dakos et al. (7), we examined metric-based indicators of tipping points in each time series. For the $[O_2]$ residuals of each time series, we estimated the statistical moments (mean, variance, skewness) and the least-square regression slope of the residuals versus time (a simple index of a linear temporal trend). Models of tipping points suggest that there should be an increase in the variance (*SI Appendix*, Fig. S16) or skewness as a break point is approached (7); evidence for CSD is best assessed by analyzing individual time series and replicate time series within each treatment (*SI Appendix, Supplemental Analysis of Time-Series Data*). We first used a randomized-block ANOVA to test for the effect of prey-addition level on each metric calculated for the entire time series (Table 1). Next, for the two highest prey-addition treatments that exhibited statistical break points, we used a matched-pairs one-sample *t* test to test for the effects of pre- vs. post-break point differences in each metric.

In addition to the break point tests and comparisons of statistical metrics, we visually examined plots of $[O_2]$ as a function of PAR (as in ref. 14). These plots trace the temporal dynamics of both variables simultaneously over the 4-d time series, and illustrate the separation of the time series into distinctive alternative states in the fed treatments. Fig. 1 illustrates residuals of $[O_2]$ as a function of PAR; *SI Appendix*, Fig. S14, illustrates the $[O_2]$/PAR relationship for raw $[O_2]$ data.

Data Availability. All raw data and R code for the analyses and mathematic code for the *Sarracenia* model are available from the Harvard Forest Data Archive (http://harvardforest.fas.harvard.edu/data-archive), dataset HF205.

ACKNOWLEDGMENTS. The authors thank Mark Van Scoy for assisting with setting up the instrumentation, Michael Lavine for discussion of statistical analyses with the corresponding author, and two anonymous reviewers and the academic editor for providing thorough and helpful comments that greatly improved the final paper. This work was supported by National Science Foundation Division of Environmental Biology Grants 11-44055 (to N.J.G.), 10-03938 (to A.M.E.), and 11-44056 (to A.M.E.).

1. Scheffer MJ, et al. (2009) Early-warning signals for critical transitions. *Nature* 461(7260):53–59.
2. Carpenter SR, et al. (2011) Early warnings of regime shifts: A whole-ecosystem experiment. *Science* 332(6033):1079–1082.
3. Carpenter SR, Brock WA (2006) Rising variance: A leading indicator of ecological transition. *Ecol Lett* 9(3):311–318.
4. Scheffer MJ, et al. (2009) *Critical Transitions in Nature and Society* (Princeton Univ Press, Princeton).
5. Contamin R, Ellison AM (2009) Indicators of regime shifts in ecological systems: What do we need to know and when do we need to know it? *Ecol Appl* 19(3):799–816.
6. Biggs R, Carpenter SR, Brock WA (2009) Turning back from the brink: Detecting an impending regime shift in time to avert it. *Proc Natl Acad Sci USA* 106(3):826–831.
7. Dakos V, et al. (2012) Methods for detecting early warnings of critical transitions in time series illustrated using simulated ecological data. *PLoS ONE* 7(7):e41010.
8. Carpenter SR, et al. (1998) Nonpoint pollution of surface waters with phosphorus and nitrogen. *Ecol Appl* 8(3):559–568.
9. Smith VH, Tilman GD, Nekola JC (1999) Eutrophication: Impacts of excess nutrient inputs on freshwater, marine, and terrestrial ecosystems. *Environ Pollut* 100(1-3): 179–196.
10. Vadeboncoeur Y, Lodge DM, Carpenter SR (2001) Whole-lake fertilization effects on distribution of primary production between benthic and pelagic habitats. *Ecology* 82(4):1065–1077.
11. Diaz RJ (2001) Overview of hypoxia around the world. *J Environ Qual* 30(2):275–281.
12. Wallace JB, Eggert SL, Meyer JL, Webster JR (1999) Effects of resource limitation on a detrital-based ecosystem. *Ecol Monogr* 69(4):409–442.
13. Lawrence D, et al. (2007) Ecological feedbacks following deforestation create the potential for a catastrophic ecosystem shift in tropical dry forest. *Proc Natl Acad Sci USA* 104(52):20696–20701.
14. Bestelmeyer BT, et al. (2011) Analysis of abrupt transitions in ecological systems. *Ecosphere* 2(12):129.
15. Scheffer M, van Nes EH (2007) Shallow lakes theory revisited: Various alternative regimes driven by climate, nutrients, depth and lake size. *Hydrobiologia* 584(1): 455–466.
16. Carpenter SR, Cottingham KL (1997) Resilience and restoration of lakes. *Cons Ecol* 1(1):2.
17. Carpenter SR, Ludwig D, Brock WA (1999) Management of eutrophication for lakes subject to potentially irreversible change. *Ecol Appl* 9(3):751–771.
18. Schröder A, Persson L, de Roos AM (2005) Direct experimental evidence for alternative stable states: A review. *Oikos* 110(1):3–19.
19. Jones HP, Schmitz OJ (2009) Rapid recovery of damaged ecosystems. *PLoS ONE* 4(5): e5653.
20. Donangelo R, et al. (2010) Early warnings for catastrophic shifts in ecosystems: Comparison between spatial and temporal indicators. *Int J Bifurcat Chaos* 20(2): 315–321.
21. Boettiger C, Hastings A (2013) Tipping points: From patterns to predictions. *Nature* 493(7431):157–158.
22. Drake JM, Griffen BD (2010) Early warning signals of extinction in deteriorating environments. *Nature* 467(7314):456–459.
23. Veraart AJ, et al. (2012) Recovery rates reflect distance to a tipping point in a living system. *Nature* 481(7381):357–359.
24. Dai L, Vorselen D, Korolev KS, Gore J (2012) Generic indicators for loss of resilience before a tipping point leading to population collapse. *Science* 336(6085):1175–1177.
25. Addicott JF (1974) Predation and prey community structure: An experimental study of the effect of mosquito larvae on the protozoan communities of pitcher plants. *Ecology* 55(3):475–492.
26. Ellison AM, et al. (2003) The evolutionary ecology of carnivorous plants. *Adv Ecol Res* 33:1–74.
27. Srivastava DS, et al. (2004) Are natural microcosms useful model systems for ecology? *Trends Ecol Evol* 19(7):379–384.
28. Bradshaw WE, Creelman RA (1984) Mutualism between the carnivorous purple pitcher plant and its inhabitants. *Am Midl Nat* 112(2):294–303.
29. Butler JL, Gotelli NJ, Ellison AM (2008) Linking the brown and green: Nutrient transformation and fate in the *Sarracenia* microecosystem. *Ecology* 89(4):898–904.
30. Farnsworth EJ, Ellison AM (2008) Prey availability directly affects physiology, growth, nutrient allocation, and scaling relationships among leaf traits in ten carnivorous plant species. *J Ecol* 96(1):213–221.
31. Schnell DE (2002) *Carnivorous Plants of the United States and Canada* (Timber Press, Portland, OR).
32. Ellison AM, Gotelli NJ (2009) Energetics and the evolution of carnivorous plants—Darwin's 'most wonderful plants in the world'. *J Exp Bot* 60(1):19–42.
33. Heard SB (1994) Pitcher plant midges and mosquitoes: A processing chain commensalism. *Ecology* 75(6):1647–1660.
34. Bledzki LA, Ellison AM (2003) Diversity of rotifers from northeastern USA bogs with new species records for North America and New England. *Hydrobiologia* 385(1-3): 193–200.
35. Baiser B, Ardeshiri RS, Ellison AM (2011) Species richness and trophic diversity increase decomposition in a co-evolved food web. *PLoS ONE* 6(5):e20672.
36. Butler JL, Atwater DZ, Ellison AM (2005) Red-spotted newts: An unusual nutrient source for northern pitcher plants. *Northeast Natural* 12(1):1–10.
37. Gotelli NJ, Ellison AM, Ballif BA (2012) Environmental proteomics, biodiversity statistics and food-web structure. *Trends Ecol Evol* 27(8):436–442.
38. Shumway RH, Stoffer DS (2011) *Time Series Analysis and Its Applications, with R Examples* (Springer, New York), 3rd Ed.
39. Cimatoribus AA, Drijfhout SS, Livina V, van der Schrier G (2012) Dansgaard-Oeschger events: Tipping points in the climate system. *Clim Past Discuss* 8(5):4269–4294.
40. Zeileis A, Leisch F, Hornik K, Kleiber C (2002) strucchange: An R package for testing for structural change in linear regression models. *J Stat Softw* 7(2):1–38.